Analysis of 2/1 locked mode disruption database from the DIII-D tokamak

R. Sweeney[1], W. Choi[1], R.J. La Haye[2], S. Mao[3,+], K.E.J. Olofsson[1,*], F.A. Volpe[1]

[1] *Columbia University, New York, NY 10027, USA*
[2] *General Atomics, San Diego, CA 92121, USA*
[3] *University of Wisconsin, Madison, WI 53706, USA*
[+] *Present address: Stanford University, Stanford, CA 94305, USA*
[*] *Present address: Oak Ridge Associated Universities, Oak Ridge, TN 37831, USA*

A database has been developed to study locked neoclassical tearing modes (NTMs) with rotating precursors and poloidal and toroidal mode numbers $m = 2$ and $n = 1$ at DIII-D. The focus of this work is to understand the nonlinear evolution of the plasma leading to a locked mode (LM) disruption, and how this differs from the evolution of a non-disruptive LM which ultimately decays or spins up. What is learned can inform disruption avoidance techniques and prediction. The 2/1 LMs are the most detrimental to plasma confinement in DIII-D and most other tokamaks [1], and are a concern for ITER [2].

Here we report on a subset of our statistical findings [3] regarding the physics of the thermal quench induced by LMs with rotating precursors, which we will sometimes refer to as "initially rotating locked modes", or IRLMs. An approximately exponential growth is observed in the final tens of milliseconds (sec. 1), followed by a sudden increase in growth rate within a few milliseconds of the thermal quench (sec. 3). The parameters l_i/q_{95} and the proximity of the island to the unperturbed plasma separatrix, referred to as d_{edge}, distinguish between disruptive and non-disruptive IRLMs, and provide insight into the physics of the disruption (sec. 2). Following the statistical results, a single thermal quench induced by a LM is presented whose qualitative characteristics are similar to tens of inspected discharges (sec. 3).

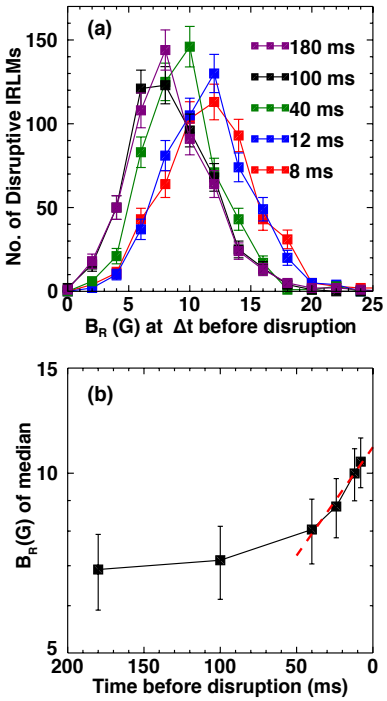

Figure 1: (a) Histograms of B_R for all disruptive IRLMs at times approaching disruption. (b) The median of the histograms in (b) on a semi-log plot. The dashed red line is fit with an e-folding time in the range [80,250] ms.

1. Median island growth preceding disruptions

Across the database, it is found that the $n = 1$ field remains approximately constant for a surprisingly long time (10 - 3000 ms) before it starts growing modestly 200 ms prior to disruption, followed by an approximate exponential growth in the last 50 ms, as shown by fig. 1. The approximately exponential growth has an e-folding time in the range $\tau_g = [80, 250]$

ms; we refer to this as the *pre-thermal quench growth*. Within $\sim$ 1 ms of the thermal quench, the growth rate increases significantly; we refer to this as the *thermal quench growth* (not shown in fig. 1, see sec. 3).

2. Distinguishing disruptive from non-disruptive IRLMs

An investigation guided by TM theory and utilizing "separation metrics" found the parameters l_i/q_{95} and d_{edge} separate disruptive from non-disruptive IRLMs best. l_i/q_{95} is the plasma internal inductance l_i divided by the safety factor at 95% of the toroidal flux q_{95}. d_{edge} is a parameter that measures the distance between the outer island separatrix and the unperturbed plasma separatrix; $d_{edge} = a - (r_{q2} + w/2)$ where a is the unperturbed plasma minor radius, r_{q2} is the minor radius of the $q = 2$ surface, and w is the island width, determined from magnetics and equilibrium data [3]. A measure of the overlap of one-dimensional probability distributions called the Bhattacharyya Coefficient (BC) [4] is used here. A BC value of 0 along a given dimension indicates a complete separation of disruptive and non-disruptive IRLMs, while a value of 1 indicates complete overlap. All BC values are evaluated at "mode end"; this is $\sim$20 ms prior to the current quench for disruptive IRLMs, and $\sim$100 ms prior to complete decay or spin-up well above the inverse wall time for non-disruptive IRLMs.

A separation of disruptive and non-disruptive IRLMs is seen in fig. 2. The quotient l_i/q_{95} separates better than either component individually according to their BC values ($\mathrm{BC}_{l_i/q_{95}} = 0.60$, $\mathrm{BC}_{l_i} = 0.84$, $\mathrm{BC}_{q_{95}} = 0.84$, all with ± 0.04 error). In a previous work [5], l_i/q_{95} is shown to be a proxy for the classical tearing stability index Δ'. It has been observed across the database that l_i increases significantly after locking, indicating a strong effect of the LM on the equilibrium current profile. It is therefore possible that a discharge with $\Delta' < 0$ transitions to a classically unstable state with $\Delta' \geq 0$ as the profile peaks, and might explain the exponential growth in fig.1.

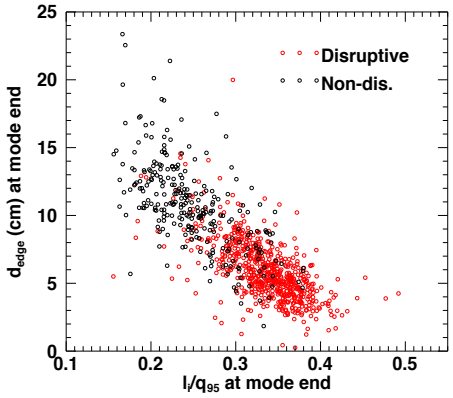

Figure 2: Disruptive and non-disruptive IRLMs are separated well in this 2D space. Low l_i/q_{95} and high d_{edge} are desirable for disruption avoidance. Note that the black points are over-plotted the red.

The d_{edge} formulation distinguishes the two classes of IRLMs better than the components alone ($\mathrm{BC}_{d_{edge}} = 0.63$, $\mathrm{BC}_{r_{q2}} = 0.70$, $\mathrm{BC}_w = 0.97$, all with ± 0.04 error). Out of parameters considered, d_{edge} also has the highest correlation $r_c = 0.47$ (albeit, only moderate) with the duration of disruptive IRLMs. The island width w alone, at ≥ 20 ms before disruption, cannot distinguish between disruptive and non-disruptive IRLMs. Indeed, simulation works [6, 7] have found that the 2/1 island separatrix nearing the cold edge of the plasma induces island growth,

ultimately leading to the thermal quench.

3. Phenomenology leading to thermal quench

In tens of discharges inspected, the thermal quench appears to be triggered by a sudden change in the electron temperature T_e profile on the inner side of the $q = 2$ surface. The time from this onset to complete collapse is typically on the order of milliseconds.

As an example, in discharge 157247, a 2/1 LM causes a disruption *during the current ramp-down*. A flattening of T_e at the $q = 2$ surface is evident in fig. 3a, in approximate agreement with estimates shown by the solid gray and blue bars based on equilibrium reconstructions and magnetics [3]. The O-point is aligned with the Electron Cyclotron Emission (ECE) [8] diagnostic at $t = 3660$ ms, and remains within $\sim 80^\circ$ toroidally throughout the disruption (see fig. 3b).

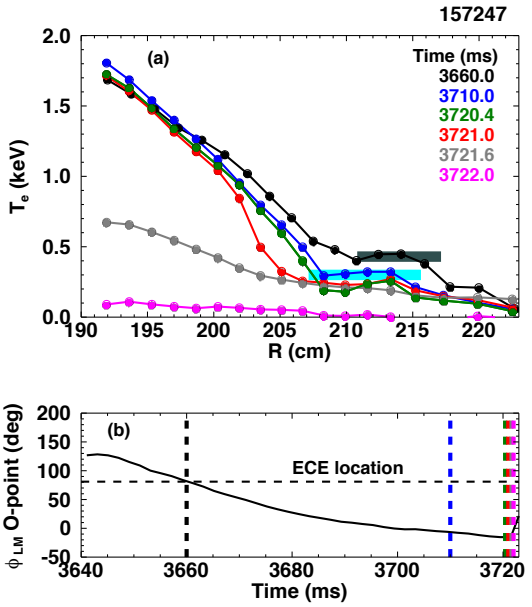

Figure 3: (a) T_e profiles from ECE prior to IRLM disruption. Horizontal bars show estimation of island position and width from magnetics and equilibrium reconstructions. (b) Toroidal position of island O-point at outboard-midplane as determined from magnetics. The horizontal line shows the location of the ECE diagnostic, vertical dashed lines show time considered in (a).

The flattening at the $q = 2$ surface grows inward and the $n = 1$ and $n = 2$ fields increase throughout the thermal quench. In the 60 ms after $t = 3660$ ms (black to green), T_e in the flattened region decreases and translates radially inward; inward translation is uncommon for disruptions *during current flattop*. In the 0.6 ms after $t = 3720.4$ ms (green to red), the flattened region grows to $\approx$7 cm. The 2/1 growth is likely not responsible for this enlargement as the $n = 1$ poloidal field $B_{\theta,1} \approx 50$ G does not change significantly between these times. However, the $n = 2$ signal increases from $B_{\theta,2} = 6$ G to 10 G, which might indicate growth of a 3/2 island at $R = 205$ cm. Just 0.6 ms later (gray), the core temperature drops; the perturbed fields also grow ($B_{\theta,1} = 80$ G, $B_{\theta,2} = 15$ G). Finally, about 1.6 ms after the thermal quench onset, the $n = 1$ and 2 fields reach 240 G and 80 G respectively, and the entire profile drops to ≤ 100 eV (magenta).

A few observations from fig. 3 are qualitatively similar to tens of IRLM disruptions inspected. Often, the width of the flat T_e region associated with the 2/1 island remains approximately constant for tens to hundreds of milliseconds before the *thermal quench growth*. This might seem in contradiction with the *pre-thermal quench growth* in fig. 1 (obtained with magnetic diagnostics). Note, however, that the width only grows by ~ 1.5 cm during the pre-thermal

quench growth, which is near the resolution limit of the ECE diagnostic. Afterwards, it grows inwards on a timescale of milliseconds, or fractions thereof. This expansion begins without any change in the core or edge T_e. The core T_e then collapses and the whole profile drops to ≤ 100 eV on a millisecond timescale. The cause of the core collapse is unknown, but core 1/1 activity likely plays a role, and might be influenced by the elevated l_i and the steepened T_e gradient outside the $q = 1$ surface caused by the 2/1 flattening.

4. Implications for disruption prediction and next steps

We have investigated the use of l_i/q_{95} and d_{edge} for disruption prediction. Unlike the data in fig. 2, disruption prediction requires considering all times. Classifying discharges with both IRLMs and $l_i/q_{95} > 0.28$ as disruptive provides 100 ms of warning time and yields $(5 \pm 1)\%$ missed IRLM disruptions and $(10 \pm 1)\%$ false alarms. Alternatively, classifying discharges with both IRLMs and $d_{edge} < 9$ cm as disruptive provides 20 ms of warning time and yields $(6 \pm 1)\%$ missed IRLM disruptions and $(10 \pm 1)\%$ false alarms. Preliminary results suggest that using a combination of l_i/q_{95} and d_{edge} in a power-law formulation might improve performance marginally. Power-law studies will be presented in a future work.

Determining the mechanism causing the sudden change in the T_e profiles inside of the $q = 2$ surface at the start of the thermal quench could provide a robust disruption prediction criterion, and possibly novel avoidance techniques. Δ' is expected to evolve significantly slower than the transition from modest to fast growth observed in the T_e profiles. However, island overlap would cause a sudden radial thermal-transport along stochastic field lines, consistent with these T_e profile observations.

This material is based upon work supported by the U.S. Department of Energy, Office of Science, Office of Fusion Energy Sciences, using the DIII-D National Fusion Facility, a DOE Office of Science user facility under awards, DE-SC0008520[1], DE-FC02-04ER54698[2], and DE-FG02-92ER54139[3]. DIII-D data shown in this paper can be obtained in digital format by following the links at https:fusion.gat.comglobal.D3D_DMP. We would like to acknowledge M. Brookman for his assistance in preparing the ECE data.

References

[1] R.J. Buttery et al. *Plasma Phys. Contr. Fusion*, 42:B61–B73, 2000.

[2] T.C. Hender, J.C. Wesley, et al. *Nucl. Fusion*, 47:S128–S202, 2007.

[3] R. Sweeney, W. Choi, et al. *arXiv*, (arXiv:1606.04183 [physics.plasm-ph]), 2016.

[4] A. Bhattacharyya. *Indian J. Statistics*, 7(4), 1946.

[5] C.Z. Cheng, H.P. Furth, and A.H. Boozer. *Plasma Phys. Contr. Fusion*, 29(3):351–366, 1987.

[6] V.A. Izzo. *Nucl. Fusion*, 46:541–547, 2006.

[7] A. Sykes and J.A. Wesson. *Phys. Rev. Lett.*, 44(18), 1980.

[8] M.E. Austin and J. Lohr. *Rev. Sci. Instrum.*, 74(3), 2003.